BAG3-dependent expression of Mcl-1 confers resistance of mutant KRAS colon cancer cells to the HSP90 inhibitor AUY922

Chun Yan Wang,[1] Su Tang Guo,[1] Amanda Croft,[1] Xu Guang Yan, [1] Lei Jin,[2] Xu Dong Zhang,[1,3] Chen Chen Jiang[2,3]

[1]School of Biomedical Sciences and Pharmacy, The University of Newcastle, NSW, 2308, Australia

[2]School of Medicine and Public Health, The University of Newcastle, NSW, 2308, Australia

[3]Correspondence: Chen Chen Jiang or Xu Dong Zhang, LS3-49, Life Sciences Building, University of Newcastle, Callaghan, NSW, Australia.

Ph: 61 2 49218906. Fax: 61 2 49217311.

Email: Chenchen.Jiang@newcastle.edu.au or Xu.Zhang@newcastle.edu.au

Running title: Mcl-1 confers resistance of colon cancer to HSP90 inhibitors

Acknowledgements

This work was supported by Cancer Council NSW, Australia (RG 16-12). C.C. Jiang and L. Jin are recipients of Cancer Institute NSW Fellowships. X.D. Zhang is supported by a Senior Research Fellowship of NHMRC.

Abbreviations

BAG3: Bcl-2-associated athanogene domain 3; EGFR: Epidermal growth factor receptor; HSP90: Heat shock protein 90; NSCLC: Non-small cell lung cancer; ER: Endoplasmic reticulum; HSF1: Heat shock factor 1; CHX: Cycloheximide.

Keywords

Colon cancer, Mcl-1, BAG3, Heat Shock Protein 90, AUY922

Abstract

Past studies have shown that mutant KRAS colon cancer cells are susceptible to apoptosis induced by the HSP90 inhibitor AUY922. Nevertheless, intrinsic and acquired resistance remains an obstacle for the potential application of the inhibitor in the treatment of the disease. Here we report that Mcl-1 is important for survival of colon cancer cells in the presence of AUY922. Mcl-1 was upregulated in mutant KRAS colon cancer cells selected for resistance to AUY922-induced apoptosis. This was due to its increased stability mediated by Bcl-2-associated athanogene domain 3 (BAG3), which was also increased in resistant colon cancer cells by heat shock factor 1 (HSF1) as a result of chronic endoplasmic reticulum (ER) stress. Functional investigations demonstrated that inhibition of Mcl-1, BAG3, or HSF1 triggered apoptosis in resistant colon cancer cells, and rendered AUY922-naïve colon cancer cells more sensitive to the inhibitor. Together, these results identify that the HSF1-BAG3-Mcl-1 signal axis is critical for protection of mutant KRAS colon cancer cells from AUY922-induced apoptosis, with potential implications for targeting HSF1/BAG3/Mcl-1 to improve the efficacy of AUY922 in the treatment of colon cancer.

Introduction

Colon cancer is one of the most common and deadly malignancies [1]. Despite recent advances in early diagnosis and the development of novel treatment approaches, the overall survival of patients with metastatic colon cancers remains disappointing [1]. This is closely related to resistance of colon cancer cells to systemic therapies resulting from oncogenic mutations of KRAS that drive activation of multiple downstream signalling pathways important for cell survival and proliferation [2]. Indeed, active mutations of KRAS are found in up to 50% of colon cancers that are predictive of intrinsic resistance to many therapeutic drugs including antibodies against the epidermal growth factor receptor (EGFR) [2,3].

Heat shock protein 90 (HSP90) is the most abundant molecular chaperone and is essential for folding, stabilization, and activation of a large number of proteins [4,5]. In particular, many mutant and overexpressed oncoproteins such as EGFR, mutant BRAF, and Akt are clients of HSP90 [6]. As such, targeting HSP90 using small molecule inhibitors appears a promising strategy in the treatment of cancer [4]. A number of HSP90 inhibitors have entered pre-clinical and clinical studies [7]. Of note, oncogene-driven cancer cells, including mutant KRAS colon cancer cells, are susceptible to HSP90 inhibition [8-10]. However, only transient responses to HSP90 inhibitors have been observed in patients with mutant KRAS tumours [11]. This is suggestive of the development of acquired resistance to HSP90 inhibitors by cancer cells [12]. Various mechanisms have been reported to be involved in acquired resistance of cancer cells to HSP90 inhibition [12-15]. For example, reactivation of the ERK-p90RSK-mTOR signalling pathway mediates acquired resistance of KRAS mutant non-small cell lung cancer (NSCLC) to the HSP90 inhibitor ganetespib [14], whereas the secondary Y142N mutation in HSP90α confers acquired resistance of MDA-MB-231 breast cancer cells to the HSP90 inhibitor PU-H71 [13]. It seems that resistance mechanisms to HSP90 inhibition may vary considerably depending on cell types and inhibitors in question.

Induction of apoptosis is a common mechanism by which therapeutic drugs kill cancer cells [16]. This is frequently mediated by activation of the mitochondrial apoptotic pathway that is regulated by the

balance between pro- and anti-apoptotic Bcl-2 family proteins [16]. Although multiple pro-apoptotic Bcl-2 family proteins are responsive to inhibition of HSP90, we have previously demonstrated that activation of the BH3-only protein Bim through the endoplasmic reticulum (ER) stress response is responsible for apoptosis of mutant KRAS colon cancer cells induced by the HSP90 inhibitor AUY922 [8]. In this study, we have examined the resistance mechanism of mutant KRAS colon cancer cells to AUY922-induced apoptosis. We report here that mutant KRAS colon cancer cells with acquired resistance to AUY922-induceded apoptosis express increased levels of the anti-apoptotic Bcl-2 family protein Mcl-1 that is critical for survival of the cells. Moreover, we show that Mcl-1 upregulation is due to its increased stability mediated by HSP70 co-chaperone Bcl-2-associated athanogene domain 3 (BAG3), which is also upregulated in mutant KRAS colon cancer cells with acquired resistance to AUY922 as a consequence of upregulation of heat shock factor 1 (HSF1) by chronic ER stress.

Materials and Methods

Cell culture

Human colon cancer cell lines provided by Professor Gordon Burns (Faculty of Health and Medicine, University of Newcastle, Australia) were described previously [17]. Individual cell line authentication was regularly confirmed every 6 months using the AmpFISTR Identifier PCR Amplification Kit from Applied Biosystems (Mulgrave, VIC, Australia) and GeneMarker V1.91 software (SoftGenetics LLC, State College, PA). The last test was carried out in February 2017.

Annexin V and Propidium Iodide staining

Staining with Annexin V and Propidium Iodide was performed as described previously [8]. In brief, cells were pelleted, washed twice with cold PBS and re-suspended in 1× binding buffer. Cells were then stained with FITC-conjugated Annexin V and PE-conjugated Propidium Iodide (BD Pharmingen™ NSW, Australia) for 15 min in the dark followed by the addition of 400 µl of binding buffer. Cells were analysed by flow cytometry within 1 hour.

Preparation of mitochondrial and cytosolic fractions

Methods used for subcellular fraction were similar to the methods previously described [18,19]. Cell pellets were suspended in five volumes of buffer A (20 mM HEPES–KOH (pH 7.5), 10 mM KCI, 1 mM Na-EGTA, 1 mM DTT, and 0.1 mM phenylmethylsulfonyl fluoride containing 250 mM sucrose) supplemented with protease inhibitor cocktail tablets. After incubation on ice for 15 min, the cells were disrupted by passing them 15 times through a 22-G needle. After centrifugation twice at 750 × *g* for 10 min at 4 °C, the supernatant was collected and centrifuged at 10 000 × *g* for 15 min at 4 °C, and the resulting mitochondrial pellets were resuspended in buffer A. The supernatants of the last spin were further centrifuged at 100 000 × *g* for 1 h at 4 °C, and the resulting supernatants were designated as the S-100 cytosolic fraction.

Three-dimensional (3D) culture

3-D culture was carried out using the hanging drop technique as previously described [8]. Briefly, 500 cells were seeded into a Perfecta3D® hanging drop plate (3D Biomatrix, Ann Arbor, MI) and allowed to grow for at least 5 days. Cells were then stained with calcein AM and ethidium homodimer-1 (Life Technologies, Scoresby, VIC, Australia) for 24 hours followed by treatment as indicated. Spheroids were harvested onto slides, and examined with the Axiovert and Axioplan microscopes (Carl Zeiss, North Ryde, NSW, Australia). Diameters of spheroids were quantified using ImageJ software (NIH, Bethesda, MD).

Plasmid vector and transfection

The pCMV6-AC-GFP-Mcl-1, pCMV6-AC-GFP-BAG3 and pCMV6-AC-GFP-HSF1 vectors were from Origene (Australian Biosearch, WA, Australia). Transfection of cDNA was carried out as described previously [8].

Immunoprecipitation

Immunoprecipitation was performed as described previously [17]. Briefly, whole cell lysates were incubated with the primary antibody or corresponding IgG for 2 hours at 4˚C, followed by incubation with 50 µl of protein A/G beads (Thermo Fisher Scientific, Scoresby, VIC, Australia). The bound proteins were eluted and processed for Western blot analysis.

Mass Spectrometry

Whole cell lysates were subject to immunoprecipitation with the anti-Mcl-1 antibody. Eluted proteins were identified using a gel-based liquid chromatography-tandem mass spectrometry (LC/MS) approach [20]. A MASCOT database search was used to visualize and validate results.

Statistical analysis and data presentation

Statistical analysis was carried out using JMP Statistics Made Visual software. Differences between different groups were assessed using Student's *t*-test. A *P* value less than 0.05 was considered

statistically significant.

Results

Mcl-1 is upregulated and is important for survival of mutant KRAS colon cancer cells with acquired resistance to AUY922

Past studies have shown that the mutant KRAS colon cancer cell lines HCT116 ($KRAS^{G13D}$) and SW480 ($KRAS^{G12V}$) are relatively sensitive to apoptosis induced by the HSP90 inhibitor AUY922 with IC50 being 76.5nM and 126nM, respectively [8]. Nevertheless, prolonged exposure of HCT116 and SW480 cells to AUY922 at their individual IC50 concentrations resulted in stable cell populations that could be passaged in the presence of the inhibitor (Fig. 1A&B). The resistant cells could also grow in medium containing AUY922 in three-dimentional (3-D) cell culture in order to imitate tumour growth *in vivo* (Fig. 1C; Fig. S1). These data indicate the successful generation of HCT116 and SW480 sublines (HCT116.R and SW480.R, respectively) resistant to AUY922-induced apoptosis. Of note, HCT116.R and SW480.R cells were cross-resistant to apoptosis induced by the structurally unrelated HSP90 inhibitor, XL888 (Fig. 1D) [21].

We examined whether anti-apoptotic Bcl-2 family proteins are involved in promoting survival of HCT116.R and SW480.R cells. Remarkably, Mcl-1 was upregulated in HCT116.R and SW480.R cells compared with their corresponding parental counterparts (Fig. 1E). In contrast, Bcl-X_L expression remained largely unaltered, whereas Bcl-2 that is a client protein of HSP90 was downregulated in HCT116.R and SW480.R cells (Fig. 1E) [20] . Silencing of Mcl-1 by shRNA triggered apoptosis that was associated with activation of caspase-3 and mitochondrial release of cytochrome C and Smac/DIABLO in HCT116.R and SW480.R cells (Figs. 1F&G; Fig. S2). Moreover, it triggered cell death in HCT116.R and SW480.R cells grown in 3-D cultures (Fig. 1H; Fig. S3). Therefore, Mcl-1 plays an important role in survival of colon cancer cells with acquired resistance to AUY922. In support, treatment with the small molecule Mcl-1 inhibitor UMI-77 similarly induced cell death in HCT116.R and SW480.R cells (Figs. 1I&J; Fig. S4) [22]. Of note, Mcl-1 silencing or treatment with UMI-77 rendered parental HCT116 and SW480 cells more sensitive to AUY922-induced apoptosis (Figs. 1K-1M). On the other hand, Overexpression of Mcl-1 protects

treatment naïve HCT116 and SW480 cells from AUY922-induced apoptosis in short-term cell viability assays and long-term clonogenic assays (Fig. S5). These data suggest that Mcl-1 also plays a role in intrinsic resistance of colon cancer cells to HSP90 inhibitors.

Improved stability of the Mcl-1 protein in colon cancer cells with acquired resistance to AUY922-induced apoptosis

Having demonstrated the functional significance of Mcl-1 in survival of colon cancer cells with acquired resistance to AUY922, we focused on investigation of the mechanism responsible for upregulation of Mcl-1 in HCT116.R and SW480.R cells. The expression levels of Mcl-1 mRNA remained comparable in HCT116.R and SW480.R cells relative to HCT116 and SW480 cells, respectively (Fig. 2A), suggesting that upregulation of Mcl-1 in HCT116.R and SW480.R cells is due to a posttranscriptional increase. Indeed, the turnover rate of Mcl-1 in HCT116.R and SW480.R cells was decelerated as shown in cycloheximide (CHX)-chase assays (Figs. 2B & 2C). Moreover, the translational rate of Mcl-1 was comparable in both parental and resistant cells (Figs. 2D & 2E) [23]. Therefore, the increase in Mcl-1 is mediated by improved stability of the protein [24]. In accordance, polyubiquitination of Mcl-1, which is required for its proteosomal degradation [24], was reduced in HCT116.R and SW480.R cells compared with their individual parental counterparts (Fig. 2F)

BAG3 is upregulated and is responsible for improved stability of Mcl-1 in HCT116.R and SW480.R cells

We carried out mass spectrometry analysis of immunoprecipitates generated with an anti-Mcl-1 antibody in total protein extracts of HCT116 and HCT116.R cells (Fig. 3A). One of the proteins with increased amount co-precipitated with Mcl-1 in HCT116.R compared with HCT116 cells was BAG3 (Figs. 3A & 3B; Fig. S6), which is a co-chaperone of HSP70 that inhibits proteasomal degradation of HSP70 client proteins including Mcl-1 [25]. Indeed, HSP70 was also one of the proteins that were increasingly co-precipitated with Mcl-1 in HCT116.R cells in the mass spectrometry analysis (Figs. 3A & 3C; Fig. S6). The increased association between Mcl-1 and BAG3 or HSP70 in HCT116.R compared with HCT116 cells was confirmed by reciprocal co-precipitation with antibodies against

BAG3 or HSP70 (Figs. 3D & 3E; Fig. S7). Similarly, there was increased association between Mcl-1 and BAG3 or HSP70 in SW480.R compared with SW480 cells (Figs. 3B-3E; Fig. S6 & S7).

We compared the expression levels of BAG3 in HCT116.R and SW480.R cells and their corresponding parental counterparts. As shown in Figure 3F, BAG3 was markedly upregulated in HCT116.R and SW480.R cells compared with HCT116 and SW480 cells, respectively, at both the protein and mRNA levels. The increase in BAG3 mRNA expression was due to a transcriptional mechanism rather than changes in its stability as its turnover rate remained comparable between resistant and parental cells as shown in actinomycin D-chasing assays (Fig. S8).

To investigate the functional significance of BAG3 in the increased stability of Mcl-1, we silenced BAG3 using two individual shRNAs in HCT116.R and SW480.R cells (Fig. 3G). Indeed, BAG3 silencing resulted in marked downregulation of Mcl-1 (Fig. 3G). This was associated with reduced stability of Mcl-1, as silencing of BAG3 shortened half-life time of the protein and increased Mcl-1 polyubiquitination (Figs. 3H & 3I; Fig. S9). In contrast, it did not alter the expression levels of Mcl-1 mRNA (Fig. 3J). Therefore, stabilization of the Mcl-1 protein by BAG3 is responsible for the increased expression of Mcl-1 in colon cancer cells resistant to AUY922. Of note, although both Mcl-1 and BAG3 were expressed at relatively low levels in HCT116 and SW480 cells, silencing of BAG3 similarly resulted in downregulation of Mcl-1 (Fig. 3K). In contrast, Overexpression of BAG3 protects treatment naïve HCT116 and SW480 cells from AUY922-triggered apoptosis in short-term cell viability assays and long-term clonogenic assays (Figs. 3L & 3M; Fig. S10). Collectively, these data indicate that BAG3 is also involved in maintaining de novo expression of Mcl-1 in colon cancer cells.

BAG3 protects colon cancer cells from apoptosis induced AUY922 through Mcl-1

Similar to silencing of Mcl-1, silencing of BAG3 induced apoptosis in HCT116.R and SW480.R cells grown in monolayer and in 3-D cultures (Figs. 4A & 4B; Fig. S11). This was due to downregulation of Mcl-1, as overexpression of Mcl-1 in HCT116.R and SW480.R cells abolished apoptosis induced by BAG3 silencing (Fig. 4C). Moreover, silencing of Mcl-1 overrides silencing of BAG3 in induction

of apoptosis in the cells (Fig. 4D). These results suggest that BAG3 upregulation plays an important role in promoting survival of colon cancer cells with acquired resistance to HSP90 inhibitors. Furthermore, silencing of BAG3, similar to silencing of Mcl-1, rendered HCT116 and SW480 cells more sensitive to AUY922-induced apoptosis (Fig. 4E), indicating that BAG3 also plays a role in intrinsic resistance of colon cancer cells to HSP90 inhibitors.

Chronic activation of the ER stress response is responsible for BAG3 upregulation through HSF1 in colon cancer cells with acquired resistance to AUY922

We have previously shown that treatment with AUY922 induces ER stress in sensitive colon cancer cells [8]. We examined whether HCT116.R and SW480.R cells have increased activation of the ER stress response. As shown in Figure 5A, the expression of GRP78 and cleaved (active) form of XBP-1 mRNA, two commonly used indicators of activation of the ER stress response [26,27], were increased in HCT116.R and SW480.R cells compared with HCT116 and SW480 cells, respectively (Fig. 5A), suggesting that colon cancer cells with acquired resistance to AUY922 have adapted to chronic ER stress.

The XBP-1 branch of the ER stress response induces the expression of the transcription factor HSF1 that is known to regulate the expression of BAG3 [28]. We therefore tested whether activation of the ER stress response is involved in upregulation of BAG3 in HCT116.R and SW480.R cells. Indeed, HSF1 expression was increased at both the protein and mRNA levels in HCT116.R and SW480.R compared with HCT116 and SW480 cells, respectively (Fig. 5B; Fig. S12), which appeared to be critical for upregulation of BAG3 and Mcl-1, as silencing of HSF1 reduced the expression of BAG3 and Mcl-1 in HCT116.R and SW480.R cells (Fig. 5C). Moreover, silencing of HSF1 triggered apoptosis (Fig. 5D). On the other hand, overexpression of HSF1 resulted in increased expression of BAG3 and Mcl-1, and protected against apoptosis induced by AUY922 in HCT116 and SW480 cells (Figs. 5E & 5F). Silencing of XBP-1 reduced the expression of HSF1 at both the protein and mRNA levels in HCT116.R and SW480.R cells, suggesting that XBP-1 is responsible for upregulation of HSF1 (Figs. 5G & 5H).

Discussion

Although a number of mechanisms have been shown to contribute to acquired resistance of mutant KRAS cancer cells to HSP90 inhibitors, such as reactivation of the ERK-p90RSK-mTOR signalling pathway and secondary Y142N mutation in HSP90α [13,14], the results in this study highlight the importance of resistance to apoptosis in determining long-term responses of mutant KRAS colon cancer cells to HSP90 inhibitors. Conceivably, upstream resistance mechanisms identified previously may converge on blockade of apoptosis. For example, activation of ERK is known to promote the expression of Mcl-1 [29], which we found in this study to be important not only for survival of colon cancer cells with acquired resistance, but also for intrinsic resistance of colon cancer cells to AUY922 [30]. Indeed, past studies have shown that AUY922 induces apoptosis in colon cancer cells through activating the BH3-only protein Bim [8], which can be bound to and antagonized by all anti-apoptotic Bcl-2 family proteins including Mcl-1 [31].

The significance of Mcl-1 in survival of colon cancer cells in the presence of AUY922 was supported by its upregulation in the cells. This made Mcl-1 distinct from the other anti-apoptotic Bcl-2 proteins, Bcl-X_L and Bcl-2. While the expression of Bcl-X_L remained unaltered, as a HSP90 client protein, Bcl-2 expression was reduced in the presence of AUY922. Intriguingly, resistance of mesothelioma and lung adenocarcinoma cells to apoptosis induced by the other HSP90 inhibitor ganetespib involves loss of Mcl-1 addiction, where inhibition of Bcl-2 reverses the resistance [32]. The relative importance of individual anti-apoptotic Bcl-2 family proteins in protection of cancer cells from HSP90 inhibition seems therefore to be cell type-dependent and is also related to the different inhibitors in question. Regardless, our results showed that colon cancer cells selected for resistance to AUY922 were cross-resistant to the structurally unrelated HSP90 inhibitor XL888 [21], emphasizing the significance of resistance to apoptosis in protection of cells from HSP90 inhibition.

Although the expression of Mcl-1 can be regulated at multiple levels [24], our results pointed to the importance of posttranslational modifications of Mcl-1 in its upregulation in colon cancer cells with acquired resistance to AUY922. Strikingly, BAG3 that has been previously shown to be important in

stabilization of Mcl-1 was co-precipitated with Mcl-1 [25], suggesting the potential involvement of BAG3 in upregulation of Mcl-1. In support, silencing of BAG3 resulted in downregulation of Mcl-1, which was associated with increased Mcl-1 polyubiquitination, shortened half-life time of the protein, and induction of apoptosis, in colon cancer cells with acquired resistance to AUY922. Moreover, silencing of BAG3 also downregulated Mcl-1 and rendered AUY922-naïve colon cancer cells more sensitive to killing by the inhibitor. Of note, although it has been reported that BAG3 inhibition similarly caused reduction in the expression of Bcl-X_L and Bcl-2 [33], we did not observe any change in the levels of Bcl-X_L and Bcl-2 expression. This was probably associated with slower rates of Bcl-X_L and Bcl-2 protein turnover in comparison with Mcl-1 [34].

Colon cancer cells carrying mutant FBW7 are reported to be resistant to inhibition of HSP90, in which mutant FBW7 fails to degrade Mcl-1 leading to Mcl-1's stabilization [35]. HCT116 and SW480 cells used in this manuscript harbour wild-type FBW7 [36]. Therefore, we believe that FBW7 may not play an important role in acquired resistance of colon cancer cells to AUY922.

Unlike other BAG family members such as BAG1 that increases HSP70 client protein degradation [37], BAG3 inhibits proteasomal degradation of HSP70 clients, which has been shown to require the interaction between BAG3 and HSP70 [38]. In accordance, BAG3 was also found to bind to HSP70, which was increased in expression, probably as a consequence of compensation for inhibition of HSP90 [39], in colon cancer cells with acquired resistance to AUY922. Of importance, BAG3 was also upregulated in resistant colon cancer cells compared with those naïve to HSP90 inhibition, further substantiating the role of BAG3 in protection of colon cancer cells against HSP90 inhibitors. In agreement with the previous finding that BAG3 is responsive to cellular stress through HSF1 [28], we found that HSF1 was upregulated, and silencing HSF1 reduced the expression of BAG3 and Mcl-1, and triggered apoptosis in colon cancer cells with acquired resistance to AUY922. Therefore, a signal axis of HSF1-BAG3-Mcl-1 is activated in colon cancer cells with prolonged exposure to AUY922 that is critical for survival of the cells.

Although HSF1 is known to be induced by inhibition of HSP90 [40], the mechanism involved remains elusive. On one hand, our past results have shown that AUY922 induces ER stress in mutant KRAS colon cancer cells [8]. On the other, induction of ER stress triggers the expression of HSF1 [41]. Indeed, colon cancer cells with acquired resistance to AUY922 displayed increased expression of GRP78 and the active form of XBP-1 mRNA, characteristic of activation of the ER stress response [26,27]. As a transcription factor, XBP-1 appeared necessary for HSF1 upregulation in resistant colon cancer cells, in that silencing of XBP-1 reduced the expression of HSF1 at both the mRNA and protein levels, in agreement with previous results on regulation of HSF1 by the ER stress response in other experimental systems [41]. Collectively, these results indicate that chronic activation of the ER stress response drives the signal pathway of HSF1-BAG3-Mcl-1 that promotes survival of colon cancer cells with acquired resistance to AUY922 (Fig. S13).

A practical implication of this study is targeting Mcl-1 to enhance the therapeutic efficacy of HSP90 inhibitors in the treatment of mutant KRAS colon cancer. Silencing of Mcl-1 kills colon cancer cells with acquired resistance to AUY922 grown in 3-D cultures, further highlighting the potential of inhibition of Mcl-1 in combination with HSP90 inhibitors *in vivo* [42]. Various Mcl-1 inhibitors are under development for the treatment of solid cancers [43,44]. Our results indicate that pre-clinical and clinical evaluations of combinations of Mcl-1 and HSP90 inhibitors are warranted. Moreover, the results also suggest that inhibition of BAG3 may be an alternative approach to improve the treatment effect of HSP90 inhibitors.

References

1. Hugen N, Brown G, Glynne-Jones R, de Wilt JH, Nagtegaal ID. Advances in the care of patients with mucinous colorectal cancer. Nat Rev Clin Oncol 2016;13(6):361-369.

2. Misale S, Yaeger R, Hobor S et al. Emergence of KRAS mutations and acquired resistance to anti-EGFR therapy in colorectal cancer. Nature 2012;486(7404):532-536.

3. Wheeler DL, Dunn EF, Harari PM. Understanding resistance to EGFR inhibitors-impact on future treatment strategies. Nat Rev Clin Oncol 2010;7(9):493-507.

4. Solit DB, Rosen N. Hsp90: a novel target for cancer therapy. Curr Top Med Chem 2006;6(11):1205-1214.

5. Goetz MP, Toft DO, Ames MM, Erlichman C. The Hsp90 chaperone complex as a novel target for cancer therapy. Ann Oncol 2003;14(8):1169-1176.

6. Whitesell L, Lindquist SL. HSP90 and the chaperoning of cancer. Nat Rev Cancer 2005;5(10):761-772.

7. Sidera K, Patsavoudi E. HSP90 inhibitors: current development and potential in cancer therapy. Recent Pat Anticancer Drug Discov 2014;9(1):1-20.

8. Wang CY, Guo ST, Wang JY et al. Inhibition of HSP90 by AUY922 Preferentially Kills Mutant KRAS Colon Cancer Cells by Activating Bim through ER Stress. Mol Cancer Ther 2016;15(3):448-459.

9. Park KS, Oh B, Lee MH et al. The HSP90 inhibitor, NVP-AUY922, sensitizes KRAS-mutant non-small cell lung cancer with intrinsic resistance to MEK inhibitor, trametinib. Cancer Lett 2016;372(1):75-81.

10. Azoitei N, Hoffmann CM, Ellegast JM et al. Targeting of KRAS mutant tumors by HSP90 inhibitors involves degradation of STK33. J Exp Med 2012;209(4):697-711.

11. Cercek A, Shia J, Gollub M et al. Ganetespib, a novel Hsp90 inhibitor in patients with KRAS mutated and wild type, refractory metastatic colorectal cancer. Clin Colorectal Cancer 2014;13(4):207-212.

12. Chai RC, Vieusseux JL, Lang BJ et al. Histone deacetylase activity mediates acquired resistance towards structurally diverse HSP90 inhibitors. Mol Oncol 2017;11(5):567-583.

13. Rouhi A, Miller C, Grasedieck S et al. Prospective identification of resistance mechanisms to HSP90 inhibition in KRAS mutant cancer cells. Oncotarget 2017;8(5):7678-7690.

14. Chatterjee S, Huang EH, Christie I, Kurland BF, Burns TF. Acquired resistance to the Hsp90 inhibitor, ganetespib in KRAS mutant NSCLC is mediated via reactivation of the ERK-p90RSK-mTOR signaling network. Mol Cancer Ther 2017.

15. Liu X, Ban LL, Luo G et al. Acquired resistance to HSP90 inhibitor 17-AAG and increased metastatic potential are associated with MUC1 expression in colon carcinoma cells. Anticancer Drugs 2016;27(5):417-426.

16. Sellers WR, Fisher DE. Apoptosis and cancer drug targeting. J Clin Invest 1999;104(12):1655-1661.

17. Guo ST, Chi MN, Yang RH et al. INPP4B is an oncogenic regulator in human colon cancer. Oncogene 2016;35(23):3049-3061.

18. Liu H, Jiang CC, Lavis CJ et al. 2-Deoxy-D-glucose enhances TRAIL-induced apoptosis in human melanoma cells through XBP-1-mediated up-regulation of TRAIL-R2. Mol Cancer 2009;8:122.

19. Lai F, Guo ST, Jin L et al. Cotargeting histone deacetylases and oncogenic BRAF synergistically kills human melanoma cells by necrosis independently of RIPK1 and RIPK3. Cell Death Dis 2013;4:e655.

20. Tuli L, Ressom HW. LC-MS Based Detection of Differential Protein Expression. J Proteomics Bioinform 2009;2:416-438.

21. Bussenius J, Blazey CM, Aay N et al. Discovery of XL888: a novel tropane-derived small molecule inhibitor of HSP90. Bioorg Med Chem Lett 2012;22(17):5396-5404.

22. Abulwerdi F, Liao C, Liu M et al. A novel small-molecule inhibitor of mcl-1 blocks pancreatic cancer growth in vitro and in vivo. Mol Cancer Ther 2014;13(3):565-575.

23. Thomas LW, Lam C, Edwards SW. Mcl-1; the molecular regulation of protein function. FEBS Lett 2010;584(14):2981-2989.

24. Juin P, Geneste O, Gautier F, Depil S, Campone M. Decoding and unlocking the BCL-2 dependency of cancer cells. Nat Rev Cancer 2013;13(7):455-465.

25. Boiani M, Daniel C, Liu X, Hogarty MD, Marnett LJ. The stress protein BAG3 stabilizes Mcl-1 protein and promotes survival of cancer cells and resistance to antagonist ABT-737. J Biol Chem 2013;288(10):6980-6990.

26. Harding HP, Calfon M, Urano F, Novoa I, Ron D. Transcriptional and translational control in the Mammalian unfolded protein response. Annu Rev Cell Dev Biol 2002;18:575-599.

27. Zhang K, Kaufman RJ. Signaling the unfolded protein response from the endoplasmic reticulum. J Biol Chem 2004;279(25):25935-25938.

28. Franceschelli S, Rosati A, Lerose R, De Nicola S, Turco MC, Pascale M. Bag3 gene expression is regulated by heat shock factor 1. J Cell Physiol 2008;215(3):575-577.

29. Boucher MJ, Morisset J, Vachon PH, Reed JC, Laine J, Rivard N. MEK/ERK signaling pathway regulates the expression of Bcl-2, Bcl-X(L), and Mcl-1 and promotes survival of human pancreatic cancer cells. J Cell Biochem 2000;79(3):355-369.

30. Wang CY, Guo ST, Wang JY et al. Reactivation of ERK and Akt confers resistance of mutant BRAF colon cancer cells to the HSP90 inhibitor AUY922. Oncotarget 2016;7(31):49597-49610.

31. Youle RJ, Strasser A. The BCL-2 protein family: opposing activities that mediate cell death. Nat Rev Mol Cell Biol 2008;9(1):47-59.

32. Busacca S, Law EW, Powley IR et al. Resistance to HSP90 inhibition involving loss of MCL1 addiction. Oncogene 2016;35(12):1483-1492.

33. Jacobs AT, Marnett LJ. HSF1-mediated BAG3 expression attenuates apoptosis in 4-hydroxynonenal-treated colon cancer cells via stabilization of anti-apoptotic Bcl-2 proteins. J Biol Chem 2009;284(14):9176-9183.

34. Mojsa B, Lassot I, Desagher S. Mcl-1 ubiquitination: unique regulation of an essential survival protein. Cells 2014;3(2):418-437.

35. Tong J, Tan S, Nikolovska-Coleska Z, Yu J, Zou F, Zhang L. FBW7-Dependent Mcl-1 Degradation Mediates the Anticancer Effect of Hsp90 Inhibitors. Mol Cancer Ther 2017;16(9):1979-1988.

36. Tong J, Tan S, Zou F, Yu J, Zhang L. FBW7 mutations mediate resistance of colorectal cancer to targeted therapies by blocking Mcl-1 degradation. Oncogene 2017;36(6):787-796.

37. Luders J, Demand J, Hohfeld J. The ubiquitin-related BAG-1 provides a link between the molecular chaperones Hsc70/Hsp70 and the proteasome. J Biol Chem 2000;275(7):4613-4617.

38. Rosati A, Graziano V, De Laurenzi V, Pascale M, Turco MC. BAG3: a multifaceted protein that regulates major cell pathways. Cell Death Dis 2011;2:e141.

39. Doong H, Rizzo K, Fang S, Kulpa V, Weissman AM, Kohn EC. CAIR-1/BAG-3 abrogates heat shock protein-70 chaperone complex-mediated protein degradation: accumulation of poly-ubiquitinated Hsp90 client proteins. J Biol Chem 2003;278(31):28490-28500.

40. Zou J, Guo Y, Guettouche T, Smith DF, Voellmy R. Repression of heat shock transcription factor HSF1 activation by HSP90 (HSP90 complex) that forms a stress-sensitive complex with HSF1. Cell 1998;94(4):471-480.

41. Luan Q, Jin L, Jiang CC et al. RIPK1 regulates survival of human melanoma cells upon endoplasmic reticulum stress through autophagy. Autophagy 2015;11(7):975-994.

42. Edmondson R, Broglie JJ, Adcock AF, Yang L. Three-dimensional cell culture systems and their applications in drug discovery and cell-based biosensors. Assay Drug Dev Technol 2014;12(4):207-218.

43. Kotschy A, Szlavik Z, Murray J et al. The MCL1 inhibitor S63845 is tolerable and effective in diverse cancer models. Nature 2016;538(7626):477-482.

44. Belmar J, Fesik SW. Small molecule Mcl-1 inhibitors for the treatment of cancer. Pharmacol Ther 2015;145:76-84.

Figure Legends:

Figure 1 – Mcl-1 is upregulated and protects against apoptosis in AUY922-resistant cells

A. HCT116, HCT116.R (left panel), SW480 and SW480.R (right panel) cells were treated with AUY922 at the indicated concentrations for 48 hours. Cell viability was quantitated using MTS assays. Data are mean ± SE, n=3. **P*<0.05, Student's *t*-test.

B. HCT116, HCT116.R, SW480 and SW480.R cells were seeded at 2000 cells/well onto 6-well plates and treated with AUY922. Cells were allowed to grow for 12 days followed with fixation with methanol and staining with crystal violet. n=3. Scale bar, 1cm.

C. Cells were plated at 500 cells/well into a 96-well Perfecta3D® Hanging drop plate. Five days later, cells were treated with AUY922 for 48 hours followed by staining with calcein AM and ethidium homodimer-1 for 30 mins. Spheroids were harvested onto a slide and images were taken with Zeiss microscope. Data are representative, n=3. Green, viable cells; Red, dead cells. Scale bar, 25μm.

D. HCT116, HCT116.R (left panel), SW480 and SW480.R (right panel) cells treated with XL888 (300nM) for 48 hours were subjected to quantitation of apoptosis by PI and Annexin V staining. Data are mean ± SE, n=3. **P*<0.05, Student's *t*-test.

E. Whole cell lysates from HCT116, HCT116.R, SW480 and SW480.R cells were subjected to Western blot analysis. Data are representative, n=3.

F. Whole cell lysates from HCT116.R and SW480.R cells transduced with control or Mcl-1 shRNAs were analysed by Western blot. Data are representative, n=3.

G. Cells transduced with the control or Mcl-1 shRNAs were subjected to quantitation of apoptosis by PI and Annexin V staining. Data are mean ± SE, n=3. ***P*<0.01, Student's *t*-test.

H. HCT116.R and SW480.R cells transduced with the control and Mcl-1 shRNA1 for 48 hours were plated at 500 cells/well onto a 96-well Perfecta3D® Hanging drop plate. Five days later, cells were stained with calcein AM and ethidium homodimer-1 for 30 mins. Spheroid cells were harvested onto a slide and images were taken with Zeiss microscope. Data are representative, n=3. Green, viable cells; Red, dead cells. Scale bar, 25μm.

I. HCT116.R and SW480.R treated with UMI-77 (20μM) for 48 hours were subjected to quantitation of apoptosis by PI and Annexin V staining. Data are mean ± SE, n=3. ***P*<0.01, Student's *t*-test.

J. HCT116.R and SW480.R cells were plated at 500 cells/ well onto a 96-well Perfecta3D® Hanging drop plate. Five days later, cells were followed treatment with UMI-77 (20μM) for 48 hours followed staining with calcein AM and ethidium homodimer-1 for 30 mins. Spheroid cells were harvested onto a slide and images were taken with Zeiss microscope. Data are representative, n=3. Green, viable cells; Red, dead cells. Scale bar, 25μm.

K. Whole cell lysates from HCT116 and SW480 cells transduced with control or Mcl-1 shRNAs were analysed by Western blot. Data are representative, n=3.

L. Cells transduced with the control or Mcl-1 shRNAs were treated with AUY922 (Individual IC50) for 48 hours. Apoptosis was measured by PI and Annexin V staining. Data are mean ± SE, n=3. **P*<0.05, ***P*<0.01, Student's *t*-test.

M. HCT116 and SW480 treated with AUY922 (individual IC50) and/or UMI-77 (20μM) for 48 hours were subjected to quantitation of apoptosis by PI and Annexin V staining. Data are mean ± SE, n=3. **P*<0.05, Student's *t*-test.

Figure 2 – Improved stability of the Mcl-1 protein in colon cancer cells with acquired resistance to AUY922-induced apoptosis

A. Total RNA from HCT116, HCT116.R, SW480 and SW480.R cells was subjected to qPCR analysis of Mcl-1 mRNA. Data are mean ± SE, n=3. Student's *t*-test.

B. Whole cell lysates from HCT116, HCT116.R, SW480 and SW480.R cells treated with CHX (cycloheximide) (10μM) for indicated time points were subjected to Western blot analysis. Data are representative, n=3.

C. Mcl-1 bands in 3 replicates of Fig. 2B were quantitated by densitometry and normalized to GAPDH; the intensity of untreated cells was arbitrarily designated as 1. Data are mean ± SE. n=3. Student's *t*-test.

D. Cells were treated with cycloheximide (10μM) for 6 hours, then cycloheximide was withdrawn before addition of MG132 (10μM) for the indicated time points. Whole cell lysates were subjected to Western blot analysis. Data are representative, n=3.

E. Mcl-1 bands in 3 replicates of Fig. 2D were quantitated by densitometry and normalized to GAPDH, the intensity of untreated cells was arbitrarily designated as 1. Data are mean ± SE. n=3. Student's *t*-test.

F. Immunoprecipitates using Mcl-1 antibody from HCT116, HCT116.R, SW480 and SW480.R treated with MG132 (10μM) for 4 hours were subjected to Western blot analysis. Data are representative, n=3.

Figure 3 – Upregulation of BAG3 is responsible for improved stability of Mcl-1 in HCT116.R and SW480.R cells

A. Representative photograph of silver stained gel from HCT116 and HCT116.R cells immunoprecipitated by using Mcl-1 antibody.

B. Whole cell lysates from HCT116, HCT116.R, SW480 and SW480.R were subjected to immunoprecipitation with the Mcl-1 antibody. The precipitates were subjected to Western blot analysis. Data are representative, n=3.

C. Whole cell lysates from HCT116, HCT116.R, SW480 and SW480.R were subjected to immunoprecipitation with the Mcl-1 antibody. The precipitates were subjected to Western blot analysis. Data are representative, n=3.

D. Whole cell lysates from HCT116, HCT116.R, SW480 and SW480.R were subjected to immunoprecipitation with the BAG3 antibody. The precipitates were subjected to Western blot analysis. Data are representative, n=3.

E. Whole cell lysates from HCT116, HCT116.R, SW480 and SW480.R were subjected to immunoprecipitation with the HSP70 antibody. The precipitates were subjected to Western blot analysis. Data are representative, n=3.

F. Left panel: Whole cell lysates from HCT116, HCT116.R, SW480 and SW480.R cells were subjected to Western blot analysis. Data are representative, n=3. Right panel: Total RNA from

HCT116, HCT116.R, SW480 and SW480.R cells was subjected to qPCR analysis of BAG3 mRNA. Data are mean ± SE, n=3. **P<0.01, Student's t-test.

G. Whole cell lysates from HCT116.R and SW480.R cells transduced with the control or BAG3 shRNAs were subjected to Western blot analysis. Data are representative, n=3.

H. Whole cell lysates from cells transfected with the control or BAG3 shRNA1 for 48 hours followed with treatment with CHX (cycloheximide) (10μM) for the indicated time points were subjected to Western blot analysis. Data are representative, n=3.

I. Whole cell lysates from cells transfected with the control or BAG3 shRNA1 for 48 hours followed by treatment with MG132 (10μM) for 4 hours were subjected immunoprecipitation with the Mcl-1 antibody. The precipitates were subjected to Western blot analysis. Data are representative, n=3.

J. Total RNA from HCT116.R and SW480.R cells transfected with the control or BAG3 shRNAs for 48 hours was subjected to qPCR analysis of Mcl-1 mRNA. Data are mean ± SE, n=3. Student's t-test.

K. Whole cell lysates from HCT116 and SW480 cells transduced with the control or BAG3 shRNAs were subjected to Western blot analysis. Data are representative, n=3.

L. Whole cell lysates from cells transduced with the control or BAG3 cDNA for 48 hours were subjected to Western blot analysis. Data are representative, n=3.

M. HCT116 (left panel) and SW480 (right panel) cells transduced with the control or BAG3 cDNA were treated with AUY922 (Individual IC50) for 48 hours. Cell viability was quantitated using MTS assays. Data are mean ± SE, n=3. *P<0.05, Student's t-test.

Figure 4 – BAG3 protects colon cancer cells from apoptosis induced AUY922 through Mcl-1

A. Cells transduced with the control or BAG3 shRNAs for 48 hours were subjected to quantitation of apoptosis by PI and Annexin V staining. Data are mean ± SE, n=3. *P<0.05, Student's t-test.

B. Cells transduced with the control or BAG3 shRNA1 for 48 hours were plated at 500 cells/well into a 96-well Perfecta3D® Hanging drop plate. Five days later, cells were stained with calcein

AM and ethidium homodimer-1 for 30 mins. Spheroids were harvested onto a slide and images were taken with Zeiss microscope. Data are representative, n=3. Green, viable cells; Red, dead cells. Scale bar, 25μm.

C. Left panel: Cells transduced with BAG3 shRNA1 were transfected with the control vector and Mcl-1 cDNA for 48 hours. Whole cell lysates were subjected Western blot analysis. Data are representative, n=3. Right panel: Cells transduced with BAG3 shRNA1 were transfected with the control vector and Mcl-1 cDNA for 48 hours. Apoptosis was measured by PI and Annexin V staining. Data are mean ± SE, n=3. $^{**}P<0.01$, Student's *t*-test.

D. HCT116.R and SW480.R cells were transduced with the control, BAG3 and/or Mcl-1 shRNA1 for 48 hours. Apoptosis was measured by PI and Annexin V staining. Data are mean ± SE, n=3. Student's *t*-test.

E. Cells transduced with the control or BAG3 shRNAs were treated with AUY922 (Individual IC50) for 48 hours. Apoptosis was measured by PI and Annexin V staining. Data are mean ± SE, n=3. $^{**}P<0.01$, $^{*}P<0.05$, Student's *t*-test.

Figure 5 – Chronic activation of the ER stress response is responsible for BAG3 upregulation through HSF1 in colon cancer cells with acquired resistance to AUY922

A. Left panel: Whole cell lysates from HCT116, HCT116.R, SW480 and SW480.R cells were subjected to Western blot analysis. Data are representative, n=3. Right panel: Total RNA from HCT116, HCT116.R, SW480 and SW480.R cells was subjected to qPCR analysis of XBP-1 mRNA. Data are mean ± SE, n=3. $^{**}P<0.01$, Student's *t*-test.

B. Left panel: Whole cell lysates from HCT116, HCT116.R, SW480 and SW480.R cells were subjected to Western blot analysis. Data are representative, n=3. Right panel: Total RNA from HCT116, HCT116.R, SW480 and SW480.R cells was subjected to qPCR analysis of HSF1 mRNA. Data are mean ± SE, n=3. $^{**}P<0.01$, $^{*}P<0.05$, Student's *t*-test.

C. HCT116.R and SW480.R cells were transduced with HSF1 shRNAs for 48 hours. Whole cell lysates were subjected Western blot analysis. Data are representative, n=3.

D. HCT116.R and SW480.R cells were transduced with control or HSF1 shRNAs for 48 hours. Apoptosis was measured by PI and Annexin V staining. Data are mean ± SE, n=3. $**P<0.01$, $*P<0.05$, Student's *t*-test.

E. Cells were transfected with vector control and HSF1 cDNA for 48 hours. Whole cell lysates were subjected Western blot analysis. Data are representative, n=3.

F. Cells were transfected with vector control and HSF1 cDNA for 24 hours followed treatment with AUY922 (individual IC50) for 48 hours. Apoptosis was measured by PI and Annexin V staining. Data are mean ± SE, n=3. $**P<0.01$, $*P<0.05$, Student's *t*-test.

G. Cells were transduced with control or XBP-1 shRNAs for 48 hours. Whole cell lysates were subjected Western blot analysis. Data are representative, n=3.

H. Total RNA from HCT116.R and SW480.R cells transduced with control or XBP1 shRNAs for 48 hours was subjected to qPCR analysis of HSF1mRNA. Data are mean ± SE, n=3. $*P<0.05$, Student's *t*-test.

Supporting Figures

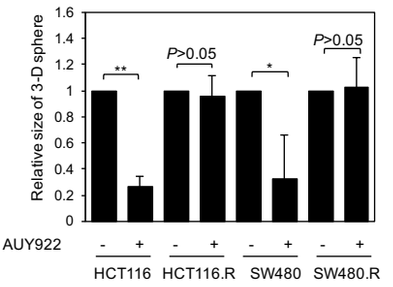

Figure S1. Relative sizes represented by relative diameters of colon cancer cell spheres as shown in Figure 1C. The diameter of the cell sphere treated with vehicle control was arbitrarily designated as 1. Data are mean ± SE, n = 3. $^{**}P < 0.01$, $^{*}P < 0.05$, Student's *t*-test.

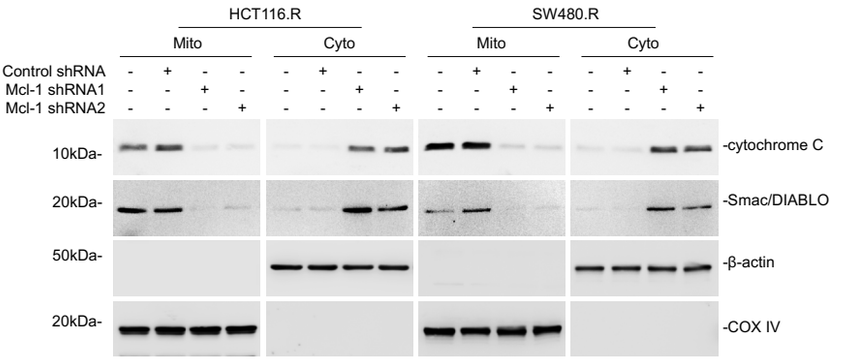

Figure S2. Silencing of Mcl-1 by shRNA triggers release of mitochondrial cytochrome C and Smac/DIABLO in HCT116.R and SW480.R cells. Mitochondrial (Mito) and cytosolic (Cyto) fractions from HCT116.R and SW480.R cells transduced with control or Mcl-1 shRNAs were subjected to Western blot analysis. Western blot analysis of COX IV and β-actin was included to show relative purity of the mitochondrial and cytosolic fractions, respectively. Data are representative, n=3.

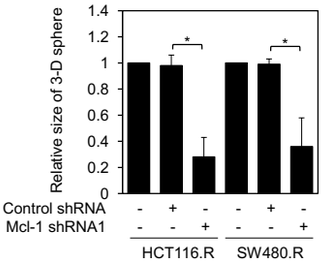

Figure S3. Relative sizes represented by relative diameters of colon cancer cell spheres as shown in Figure 1H. The diameter of the cell sphere transduced with control shRNA was arbitrarily designated as 1. Data are mean ± SE, n = 3. *$P < 0.05$, Student's *t*-test.

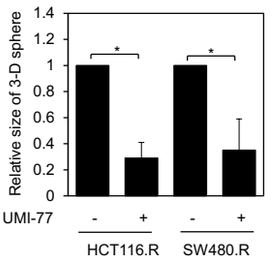

Figure S4. Relative sizes represented by relative diameters of colon cancer cell spheres as shown in Figure 1J. The diameter of the cell sphere treated with vehicle control was arbitrarily designated as 1. Data are mean ± SE, n = 3. **P* < 0.05, Student's *t*-test.

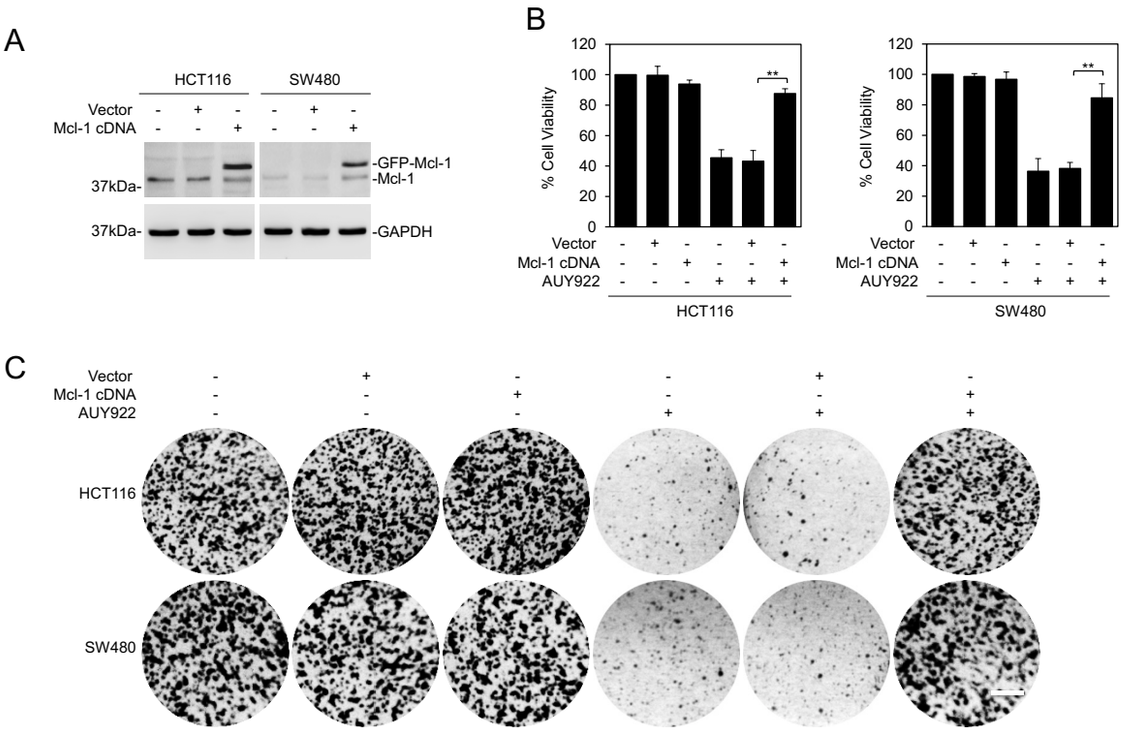

Figure S5. Overexpression of Mcl-1 protects HCT116 and SW480 parental cells from AUY922-meidated apoptosis. HCT116 and SW480 cells were transfected with the control or Mcl-1 cDNA. A**,** Whole cell lysates from cells transduced with the control or Mcl-1cDNA for 48 hours were subjected to Western blot analysis. Data are representative, n=3.

B, Cells were treated with AUY922 (Individual IC50) for 48 hours. Cell viability was quantitated using MTS assays. Data are mean ± SE, n=3. ***P*<0.01, Student's *t*-test. C**,** Cells were seeded at 2000 cells/well onto 6-well plates and treated with AUY922 for 12 days followed with fixation with methanol and staining with crystal violet. Data are representative, n=3. Scale bar, 1cm.

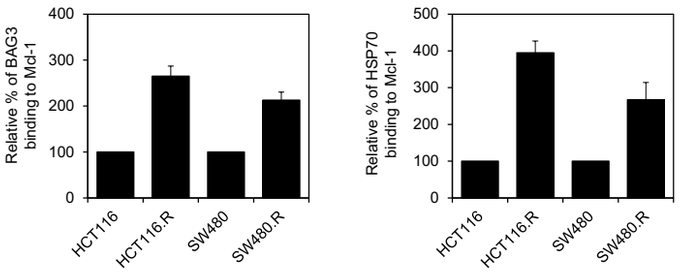

Figure S6. The relative percentage of BAG3 or HSP70 binding to Mcl-1 in resistant cells is increased compared with parental cells. Mcl-1 and BAG3 or HSP70 bands in 3 replicates of Fig. 3B or C were quantitated by densitometry and normalized to GAPDH, the intensity of BAG3 or HSP70 binding to Mcl-1 in untreated cells was arbitrarily designated as 1. Data are mean ± SE. n=3. Student's *t*-test.

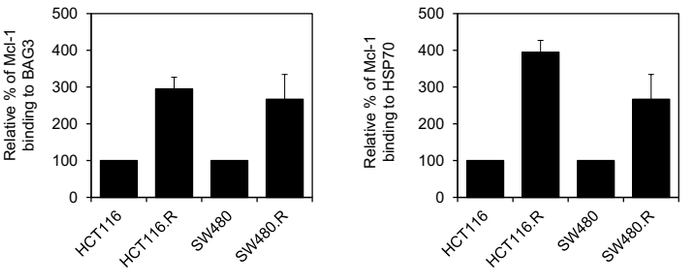

Figure S7. The relative percentage of Mcl-1 binding to BAG3 or Mcl-1 binding to HSP70 in resistant cells is increased compared with parental cells. Mcl-1, BAG3 or HSP70 bands in 3 replicates of Fig. 3D or E were quantitated by densitometry and normalized to GAPDH, the intensity of Mcl-1 binding to BAG3 or HSP70 in untreated cells was arbitrarily designated as 1. Data are mean ± SE. n=3. Student's *t*-test.

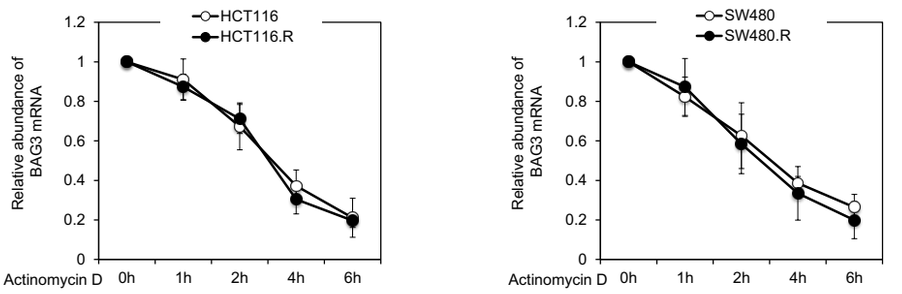

Figure S8. The increase in BAG3 mRNA expression is not due to the change in its stability
HCT116 and HCT116.R (Left) or SW480 and SW480.R (right) cells treated with AUY922 (Individual IC50) in the present of actinomycin D (10μg/ml) for the indicated intervals were subjected to qPCR analysis of BAG3 mRNA. Data are mean ± SE, n=3, Student's *t*-test.

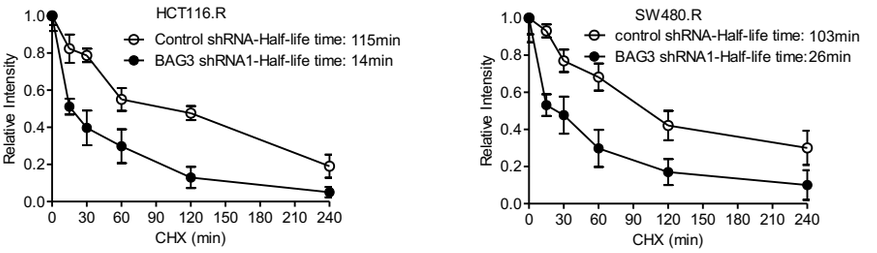

Figure S9. Silencing of BAG3 shortens half-life time of the Mcl-1 protein
Mcl-1 bands in 3 replicates of Fig. 3H were quantitated by densitometry and normalized to GAPDH, the intensity of untreated cells was arbitrarily designated as 1. Data are mean ± SE. Student's *t*-test.

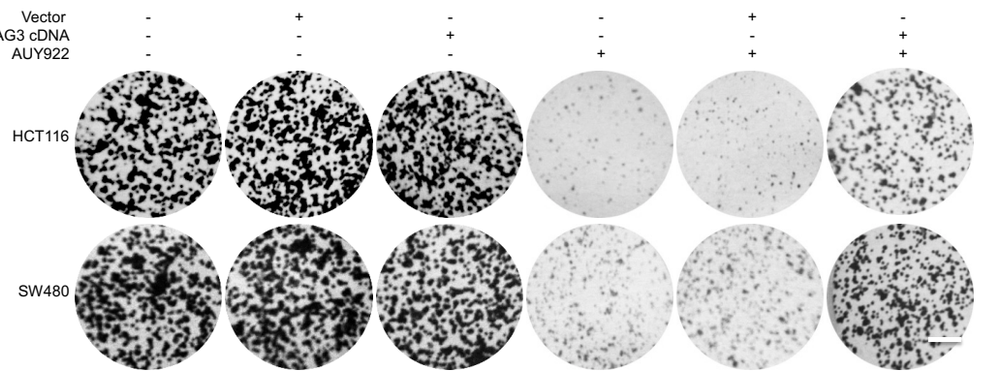

Figure S10. Overexpression of BAG3 protects HCT116 and SW480 parental cells from AUY922-meidated apoptosis. HCT116 and SW480 cells were transfected with the control or BAG3 cDNA. Cells were seeded at 2000 cells/well onto 6-well plates and treated with AUY922 for 12 days followed with fixation with methanol and staining with crystal violet. Data are representative, n=3. Scale bar, 1cm.

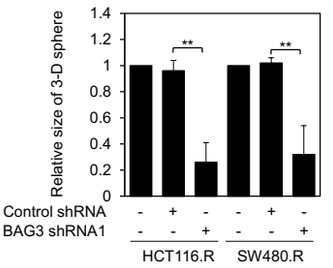

Figure S11. Relative sizes represented by relative diameters of colon cancer cell spheres as shown in Figure 4B. The diameter of the cell sphere transduced with control shRNA was arbitrarily designated as 1. Data are mean ± SE, n = 3. $^{**}P < 0.01$, Student's *t*-test.

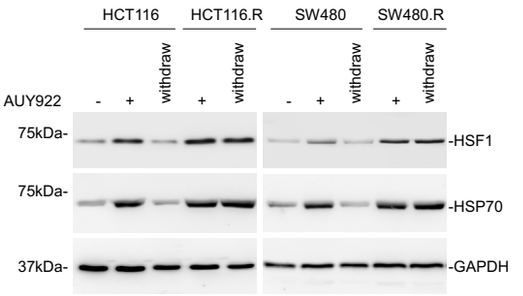

Figure S12. Withdraw of AUY922 for 16 hours does not result in changes in the expression of HSF1 and HSP70 in the resistant cells; however, it abolishes AUY922-mediated upregulation of HSF1 and HSP70 in parental cells. Whole cell lysates from HCT116, HCT116.R, SW480 and SW480.R cells treated with AUY922 for 48 hours following withdraw of AUY922 for 16 hours were subjected to Western blot analysis. Data are representative, n=3.

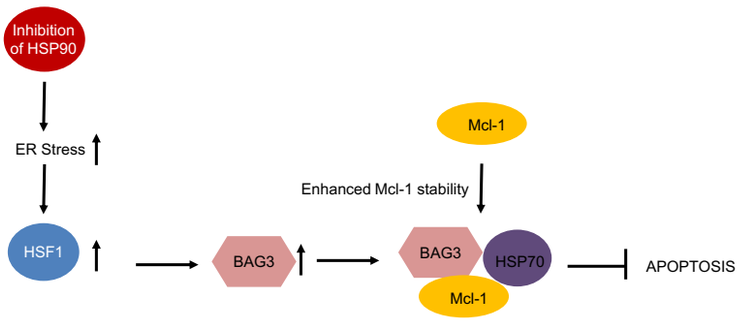

Figure S13. A schematic illustration of the resistant mechanism of colon cancer cells to HSP90 inhibitors. Inhibition of HSP90 induces ER stress, which results in upregulation of HSF1. The increased expression of HSF1 is responsible for upregulation of BAG3, which binds to and stabilizes Mcl-1, consequently, leading to inhibition of apoptosis.

Supporting materials and methods

Antibody and reagents

Antibodies against HSP70 (4872), PUMA (4976), HSF1 (4356) and ubiquitin (P4D1) (3936) were from Cell Signalling Technology (Beverly, MA. Antibodies against Mcl-1 (sc-12756), Bcl-2 (sc-7382), Bcl-X_L (sc-8392), GRP78 (sc-13968) and XBP-1 (sc-7160) were purchased from Santa Cruz Biotechnology (Santa Cruz, CA). Antibody against caspase-3 (AAP-113) was purchased form Enzo Life Sciences (Dural, NSW, Australia). Antibodies against BAG3 (NOVNBP227398) were purchased from Novus (Noble Park North,VIC, Australian). Antibodies used for BAG3 (ab47124) and HSP70 (ab5439) IP were purchased from Abcam (Cambridge, MA). Antibody used for Mcl-1 (559027) IP were purchased from BD Biosciences (San Jose, CA). AUY922, UMI-77 and XL888 were provided by Selleckchem (Redfern, NSW, Australia).

Cell viability assays (MTS assays)

Cell viability was quantitated using VisionBlue Fluorescence Cell Viability Assay Kit (Biovision Inc., Mountain View, CA, USA) as described previously [3]. Briefly, cells were seeded at 5000 cells per well onto flat-bottomed 96-well culture plates and allowed to grow for 24 h followed by the desired treatment. Cells were then labeled with the VisionBlue reagent and detected by Synergy two multi-detection microplate reader (BioTek, Winooski, VT, USA) according to the manufacturer's instructions.

Real-time PCR

qPCR was performed as described previously [1]. The primer sequences used are: Mcl-1 forward, 5'-GGAAGGCGCTGGAGACCTTA-3', reverse, 5'-CAACGATTTCACATCGTCTTCGT-3'; BAG3 forward, 5'- AGCCCATGACCCATCGAGAA -3', reverse, 5'- CCACCTCTTTGCGGATCACT-3'; XBP-1 forward, 5'-AGCCAAGGGGAATGAAGTGAG-3', reverse, 5'-CTGCAGAGGTGCACGTAGTC-3'; HSF1 forward, 5'- GGAAGGCGCTGGAGACCTTA-3',

reverse, 5'-CAACGATTTCACATCGTCTTCGT-3'. The relative abundance of target mRNA in control group was arbitrarily designated as 1.

Clonogenic assays

Clonogenic assays were carried out as described previously [2]. In brief, 2000 cells/well were seeded onto 6-well culture plates. Cells were then incubated for a further 12 days before staining with crystal violet (0.5% solution). Colonies with 50 or more cells were calculated under a phase contrast microscope.

shRNA

SMARTvector Lentiviral Humanm Mcl-1 shRNA-1 (V3SH11243-00EG4170), Mcl-1 shRNA-2 (Mcl-1 shRNA-1 (V3SH11243-00EG4170), BAG3 shRNA-1 (V3SH11243-00EG9531), BAG3 shRNA-2(V3SH11240-225636297), HSF1 shRNA-1 (V3SH11240-23037027), HSF1 shRNA-2 (V3SH11240-230238739), XBP-1 shRNA-1 (V3SH11243-00EG7494) and XBP-1 shRNA-2 (V3SH11240-224864159) the control particles were from Dharmacon (Millennium Science Pty Ltd., Mulgrave, VIC, Australia). Transduction of shRNA was carried out as described previously [3].

Western blotting

Western blot was performed as described previously [4]. Targeted bands were detected by Immun-Star^{TM} HRP Chemiluminescent Kit, and images were captured and the intensity of the bands was quantitated with the Bio-Rad VersaDoc^{TM} image system (Bio-Rad, Regents Park, NSW, Australia).

Supporting References

1. Jiang CC, Lucas K, Avery-Kiejda KA, et al. Up-regulation of Mcl-1 is critical for survival of human melanoma cells upon endoplasmic reticulum stress. Cancer Res 2008;68(16):6708-6717.

2. Wang CY, Guo ST, Wang JY, et al. Inhibition of HSP90 by AUY922 Preferentially Kills Mutant KRAS Colon Cancer Cells by Activating Bim through ER Stress. Mol Cancer Ther 2016;15(3):448-459.

3. Guo ST, Chi MN, Yang RH, et al. INPP4B is an oncogenic regulator in human colon cancer. Oncogene 2016;35(23):3049-3061.

4. Ye Y, Jin L, Wilmott JS, et al. PI(4,5)P2 5-phosphatase A regulates PI3K/Akt signalling and has a tumour suppressive role in human melanoma. Nat Commun 2013;4:1508.

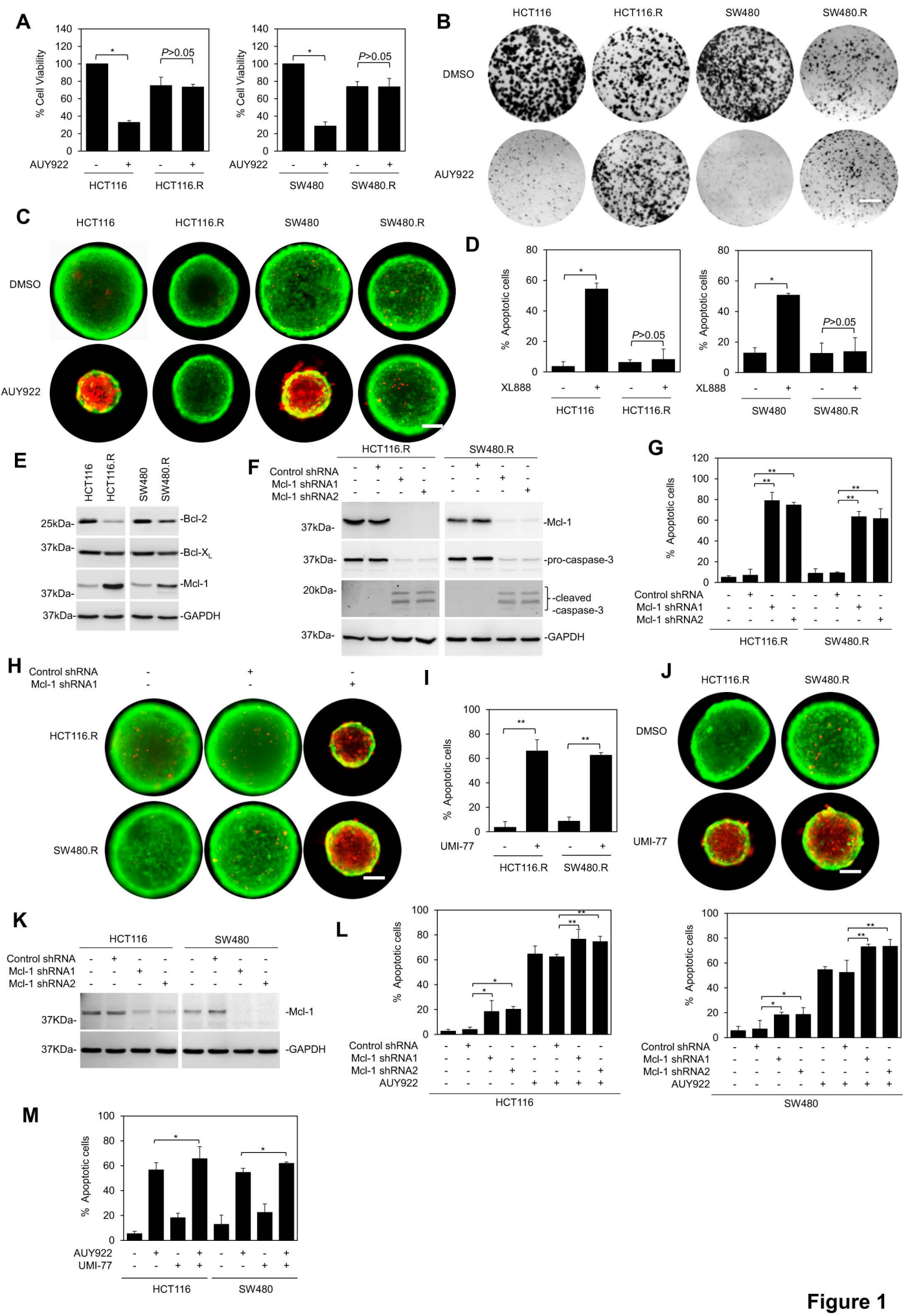
A
% Cell Viability
AUY922
HCT116
HCT116.R
SW480
SW480.R
P>0.05
B
DMSO
AUY922
C
D
% Apoptotic cells
XL888
E
25kDa-
-Bcl-2
37kDa-
-Bcl-XL
-Mcl-1
-GAPDH
F
Control shRNA
Mcl-1 shRNA1
Mcl-1 shRNA2
20kDa-
-cleaved
-caspase-3
-pro-caspase-3
G
H
I
UMI-77
J
K
37KDa-
L
M

Figure 1

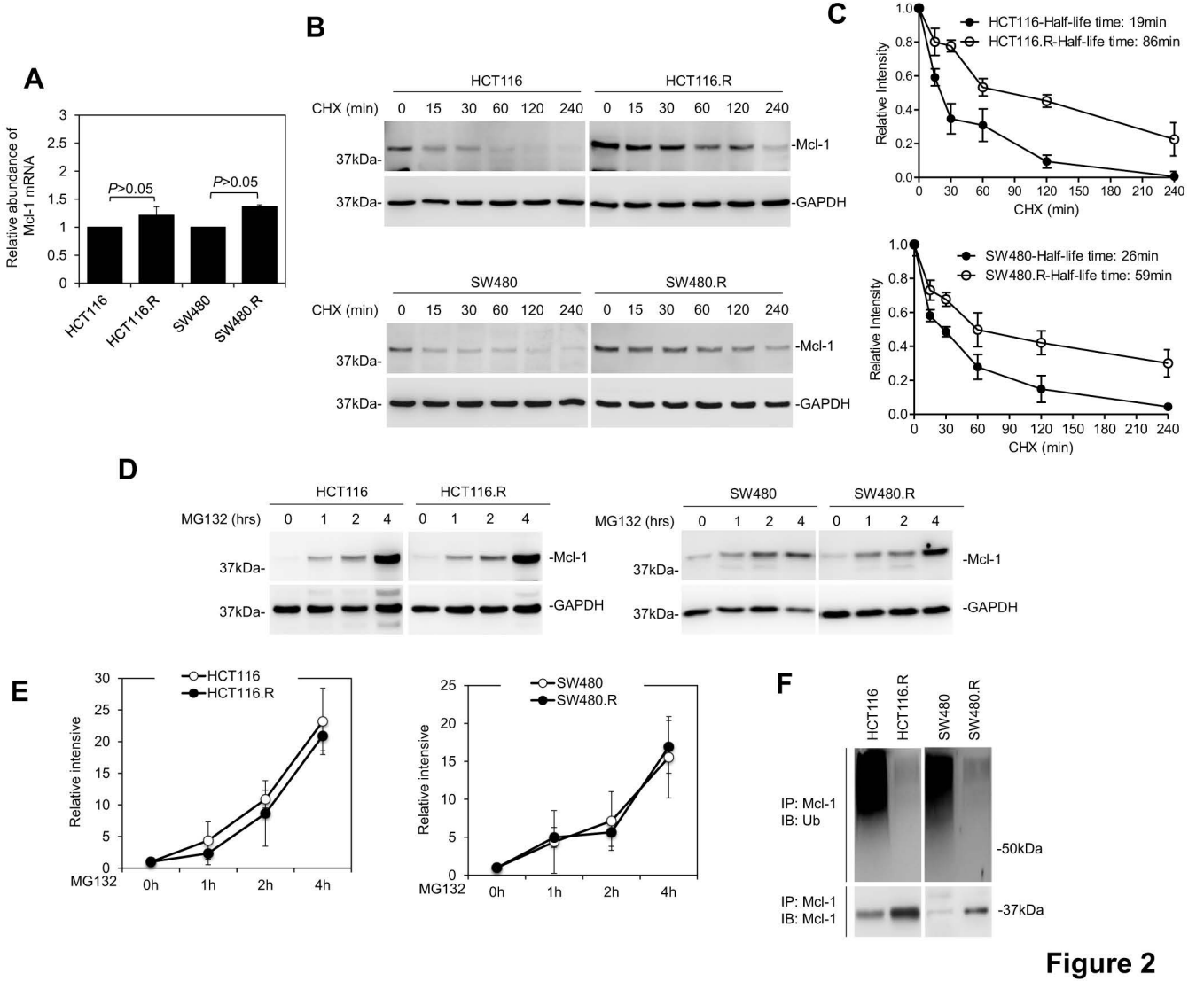
A
Relative abundance of Mcl-1 mRNA
P>0.05
P>0.05
HCT116
HCT116.R
SW480
SW480.R
B
HCT116
HCT116.R
CHX (min) 0 15 30 60 120 240 0 15 30 60 120 240
37kDa-
-Mcl-1
37kDa-
-GAPDH
SW480
SW480.R
CHX (min) 0 15 30 60 120 240 0 15 30 60 120 240
37kDa-
-Mcl-1
37kDa-
-GAPDH
C
HCT116-Half-life time: 19min
HCT116.R-Half-life time: 86min
Relative Intensity
CHX (min)
SW480-Half-life time: 26min
SW480.R-Half-life time: 59min
Relative Intensity
CHX (min)
D
HCT116
HCT116.R
MG132 (hrs) 0 1 2 4 0 1 2 4
37kDa-
-Mcl-1
37kDa-
-GAPDH
SW480
SW480.R
MG132 (hrs) 0 1 2 4 0 1 2 4
37kDa-
-Mcl-1
37kDa-
-GAPDH
E
HCT116
HCT116.R
Relative intensive
MG132 0h 1h 2h 4h
SW480
SW480.R
Relative intensive
MG132 0h 1h 2h 4h
F
HCT116
HCT116.R
SW480
SW480.R
IP: Mcl-1
IB: Ub
-50kDa
IP: Mcl-1
IB: Mcl-1
-37kDa

Figure 2

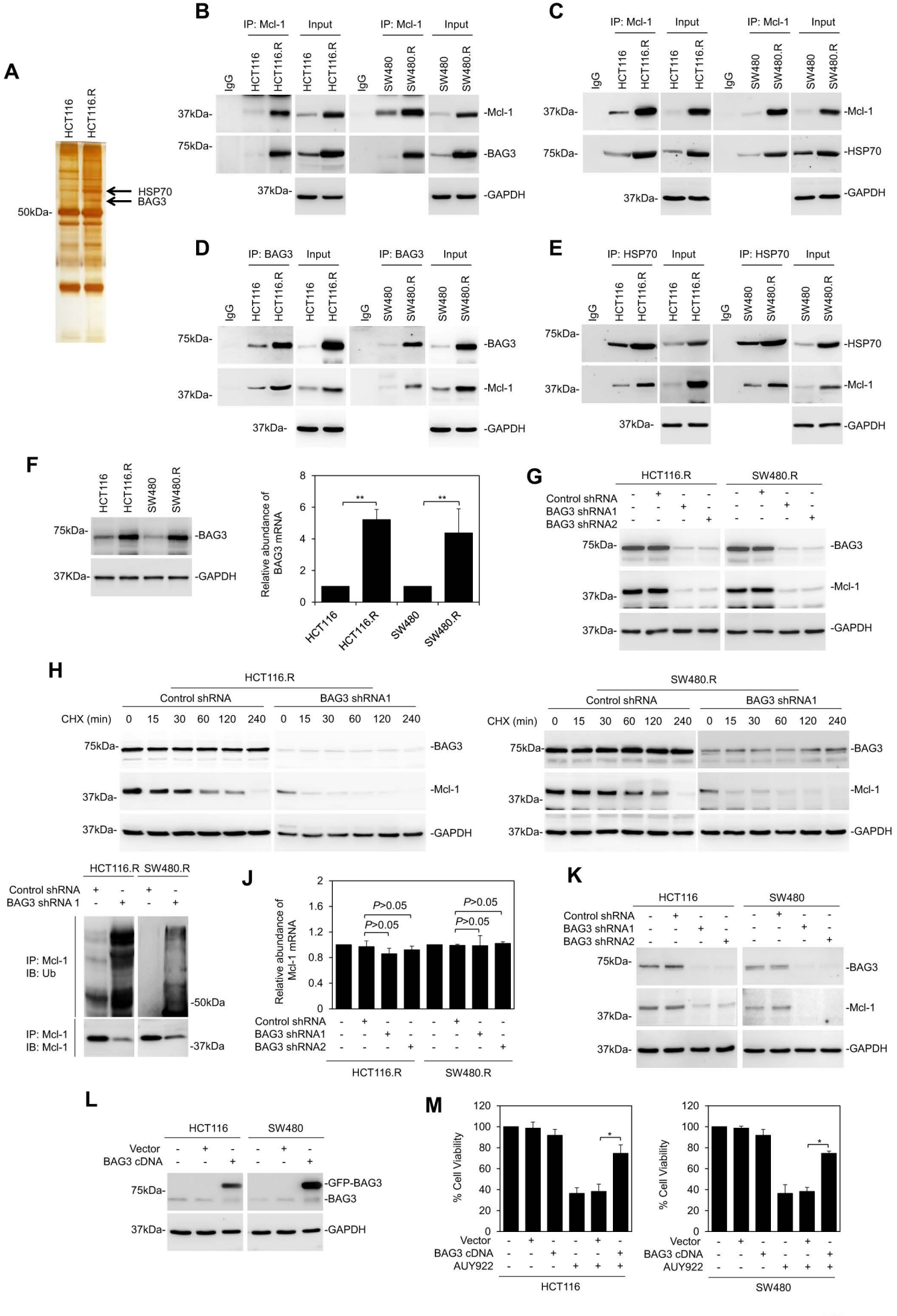
A
HCT116
HCT116.R
HSP70
BAG3
50kDa-
B
IP: Mcl-1
Input
IgG
HCT116
HCT116.R
SW480
SW480.R
37kDa-
75kDa-
-Mcl-1
-BAG3
-GAPDH
C
-HSP70
D
IP: BAG3
E
IP: HSP70
F
37KDa-
Relative abundance of BAG3 mRNA
**
G
Control shRNA
BAG3 shRNA1
BAG3 shRNA2
H
CHX (min)
0 15 30 60 120 240
I
IP: Mcl-1
IB: Ub
IB: Mcl-1
-50kDa
-37kDa
J
Relative abundance of Mcl-1 mRNA
P>0.05
K
L
Vector
BAG3 cDNA
-GFP-BAG3
-BAG3
M
% Cell Viability
AUY922
*

Figure 3

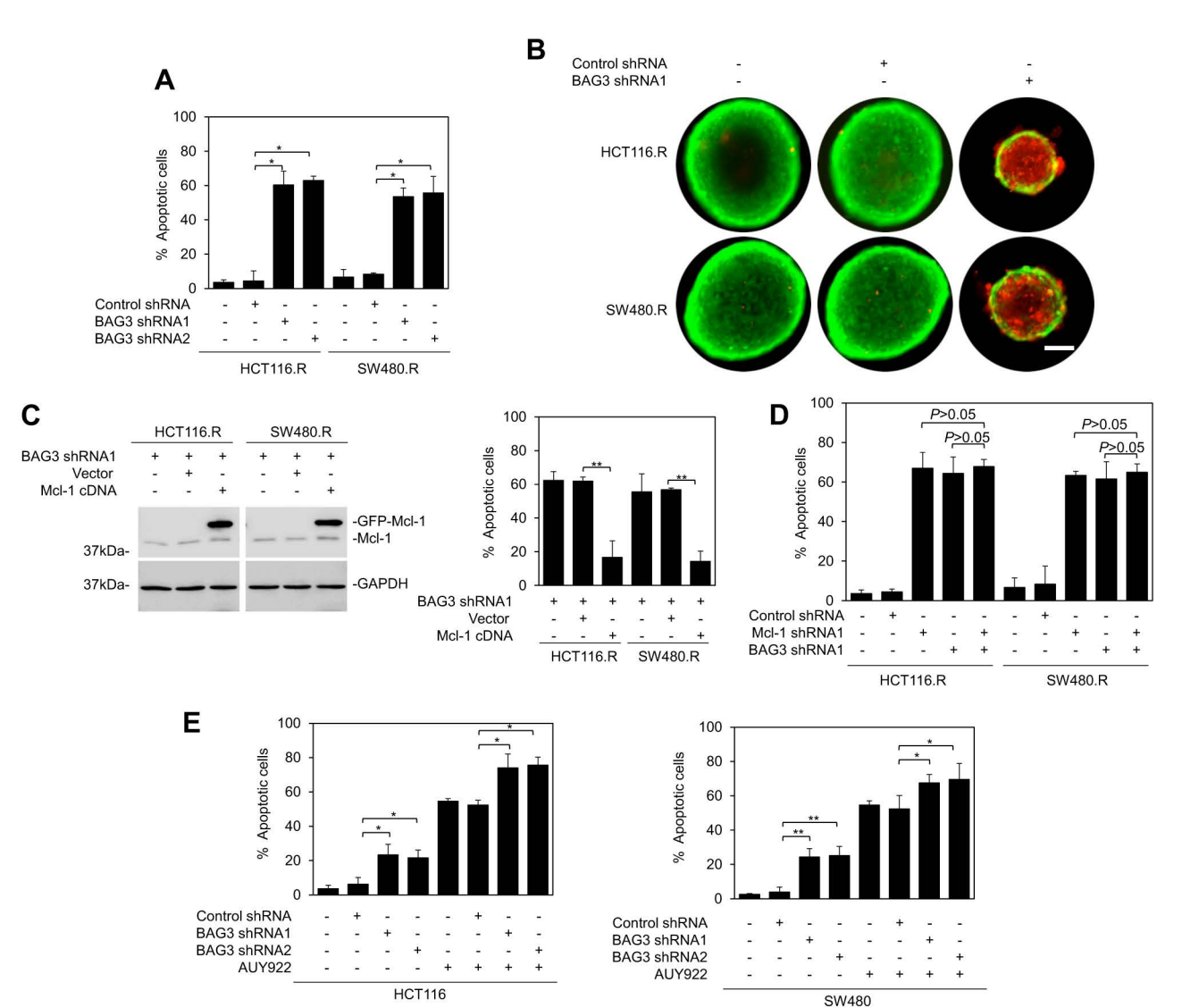
A
% Apoptotic cells
Control shRNA
BAG3 shRNA1
BAG3 shRNA2
HCT116.R
SW480.R
B
Control shRNA
BAG3 shRNA1
HCT116.R
SW480.R
C
HCT116.R
SW480.R
BAG3 shRNA1
Vector
Mcl-1 cDNA
-GFP-Mcl-1
-Mcl-1
37kDa-
37kDa-
-GAPDH
% Apoptotic cells
D
% Apoptotic cells
P>0.05
Control shRNA
Mcl-1 shRNA1
BAG3 shRNA1
E
% Apoptotic cells
Control shRNA
BAG3 shRNA1
BAG3 shRNA2
AUY922
HCT116
SW480

Figure 4

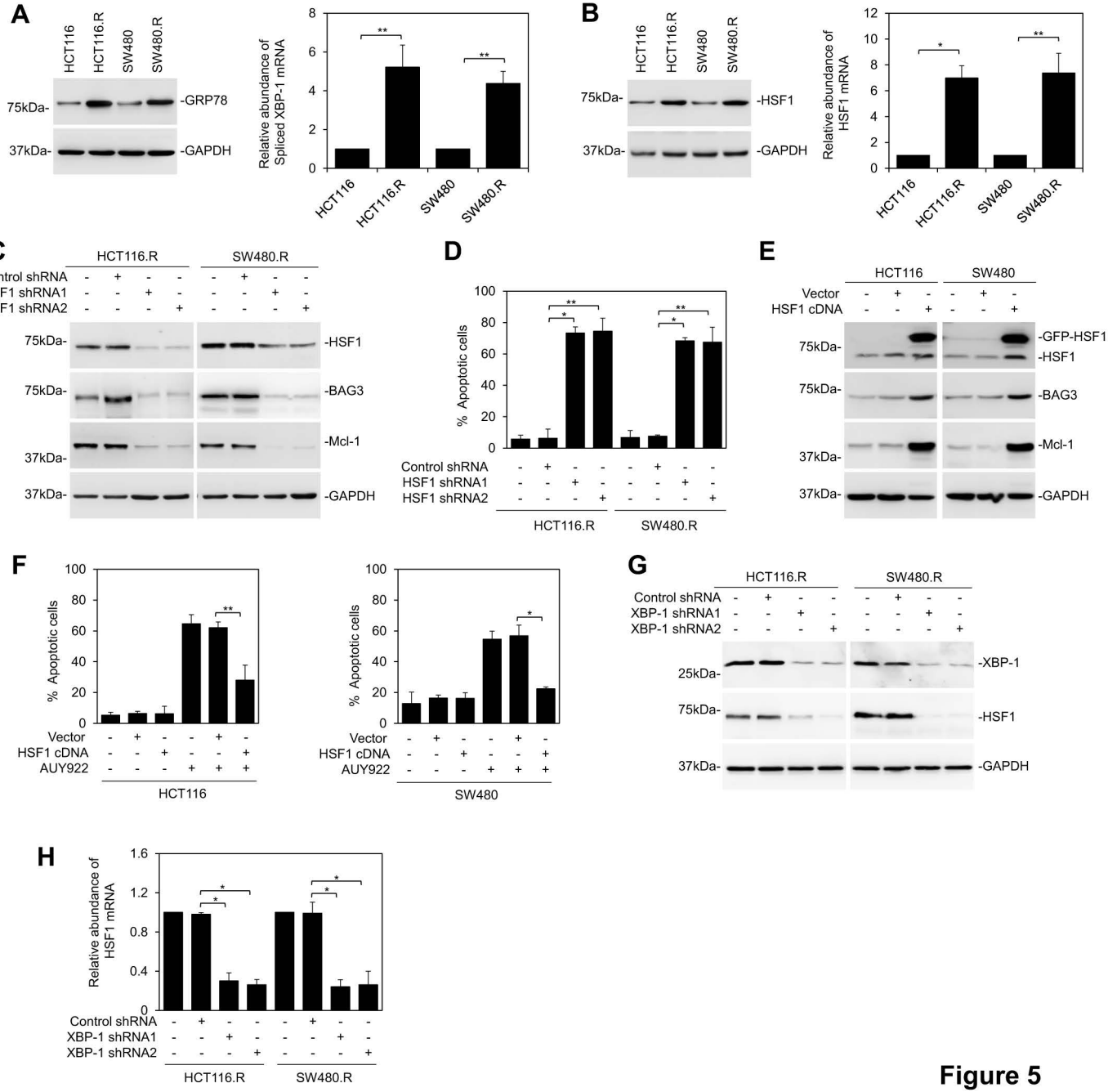
A
HCT116
HCT116.R
SW480
SW480.R
75kDa-
-GRP78
37kDa-
-GAPDH
Relative abundance of Spliced XBP-1 mRNA
B
-HSF1
Relative abundance of HSF1 mRNA
C
HCT116.R
SW480.R
Control shRNA
HSF1 shRNA1
HSF1 shRNA2
-HSF1
-BAG3
-Mcl-1
D
% Apoptotic cells
E
Vector
HSF1 cDNA
-GFP-HSF1
F
AUY922
G
XBP-1 shRNA1
XBP-1 shRNA2
25kDa-
-XBP-1
H

Figure 5